

***In situ* x-ray diffraction study of the size dependence of pressure-induced structural transformation in amorphous silica nanoparticles**

Takashi Uchino,¹ Atsuko Aboshi,¹ Tomoko Yamada,¹ Yasuhiro Inamura,² and Yoshinori Katayama²
¹*Department of Chemistry, Kobe University, Kobe 657-8501, Japan*

²*Synchrotron Radiation Research Center, Japan Atomic Energy Research Institute, Sayo, Hyogo 679-5198, Japan*

(Received 12 March 2008; published 9 April 2008)

An x-ray diffraction study of nanometer-sized amorphous silica particles was carried out at pressures of up to 7.4 GPa by using an energy dispersive synchrotron-radiation technique. We found that silica nanoparticles exhibit pressure-induced structural changes, which eventually lead to a permanent densification, at much lower pressures than what occurs in a bulk silica glass. Decreasing the size hence provides a new window for amorphous-amorphous transformations and also implies the appearance of a first-order-like, or thermodynamically controlled, transition pathway, even at room temperature.

DOI: [10.1103/PhysRevB.77.132201](https://doi.org/10.1103/PhysRevB.77.132201)

PACS number(s): 61.46.-w, 61.05.cc, 61.43.Fs, 62.50.-p

There has been an ongoing interest in the nature of structural transformations in topologically disordered systems under high pressure in view of the transitions between low-density liquid and high-density liquid and between low-density amorphous (LDA) and high-density amorphous (HDA).¹⁻⁷ It is believed that the observed transitions that occur at a constant composition derive from a minimization of the free energy in response to the pressure or temperature. Density and entropy differences between HDA and LDA are indeed found in amorphous ice systems, and the pressure-induced structural transitions result from first-order thermodynamic transformations.⁵ In addition to pressure and temperature, here we show that size can also be an important variable in determining the transformation behaviors of amorphous solids on the basis of high-pressure x-ray diffraction experiments on amorphous silica (*a*-SiO₂) nanoparticles. In crystalline materials, the size dependence of a solid-solid phase transition has been widely investigated.⁸⁻¹³ Some crystalline materials⁸⁻¹⁰ show a higher phase transformation pressure with decreasing size, but others¹¹⁻¹³ exhibit the opposite behavior, depending on the surface energy term between the phases involved in the material. However, the size dependence of pressure-induced transformations in amorphous solids has not been fully investigated and analyzed.

a-SiO₂ is one of the most well studied disordered materials in terms of both theoretical and experimental approaches. Thus far, the effects of pressure and temperature on the short-range (~0.2–~0.5 nm) and intermediate-range (~0.5–~2 nm) structures of bulk silica glass have been extensively investigated.¹⁴⁻¹⁸ It has been well documented that the compression of bulk silica glass at room temperature is reversible at pressures below ~10 GPa, indicating little or no bond breaking and network rearrangement in this pressure region. At pressures between ~10 and ~20 GPa, the compression is irreversible and is accompanied by a permanent densification at room temperature. The phenomenon is often called a “polyamorphic” transformation.⁴ It is also interesting to note that higher temperatures can lead to a much greater densification for a given pressure; the onset pressure of a permanent densification can be lowered down to ~5 GPa by increasing the temperature to as high as ~600 °C.^{19,20} This indicates that thermally activated atomic

rearrangements play a vital role in pressure-induced structural transformations, even far below the glass transition temperature. In our previous paper,²¹ we reported that in *a*-SiO₂ nanoparticles with a primary particle size of 7 nm, anelastic compression can occur at room temperature after releasing the pressure from 4 to 8 GPa, which is well below the pressure regime of the anelastic compression (~10–~20 GPa) that is observed for bulk silica glass. In this Brief Report, we carry out *in situ* x-ray diffraction measurements at pressures of up to 7.4 GPa at room temperature to get further knowledge about the size dependence of pressure-induced structural transformations on *a*-SiO₂. We then discuss the effect of particle size on the thermodynamic and kinetic stabilities of *a*-SiO₂ and the related polyamorphic transformation.

A cubic-type multianvil apparatus installed on the BL14B1 beamline at the SPring-8 synchrotron radiation facility was used for the *in situ* x-ray diffraction experiments.⁶ Amorphous silica nanoparticles used in this work were the so-called fumed silica (S-5130 from Sigma) with a primary particle size of 7 nm, which is produced at high temperatures of about 1200–1600 °C by the hydrolysis of silicon tetrachloride vapor in an oxygen-hydrogen flame. The true density of the fumed silica aggregate (2.20 g/cm³) is the same as that of normal bulk silica glass,²² indicating that fumed silica consists of nonporous, dense silica nanoparticles. The amount of adsorbed H₂O and CO₂ molecules along with surface hydroxyl groups was kept as low as possible by heating the particles at 1000 °C for 3 h in air.²³ The x-ray diffraction pattern was measured by an energy-dispersive method. Diffraction data were collected at eight different scattering angles within the range 3° < 2θ < 16° at pressures of up to 7.4 GPa by using white x rays with energies of 20–170 keV. The diffraction data that are obtained at each angle were then combined and averaged to form a single structure factor *S*(*Q*). Each applied pressure was calibrated from the lattice constant of NaCl that was intentionally added to the sample.

Figure 1 shows *S*(*Q*) of *a*-SiO₂ nanoparticles for the series of applied pressures. At ambient pressure, *S*(*Q*) of *a*-SiO₂ nanoparticles is essentially identical to that of the bulk silica glass, which is in agreement with previous high-energy x-ray scattering experiments on fumed silica.²³ These

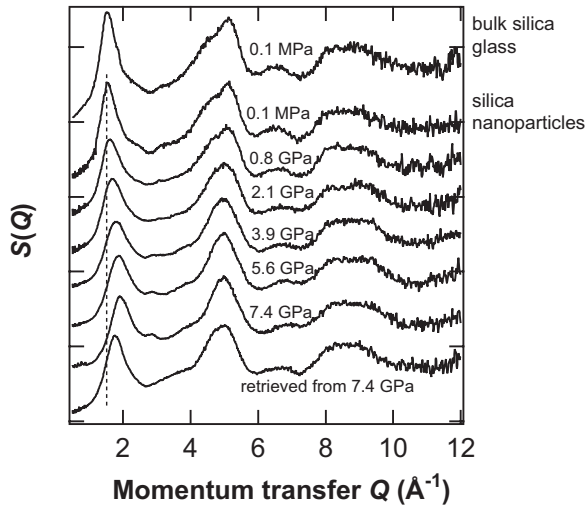


FIG. 1. The x-ray structure factor $S(Q)$ measured for amorphous silica nanoparticles between 0.1 MPa and 7.4 GPa and that of the pressure retrieved sample from 7.4 GPa. The data for bulk silica glass at ambient pressure (Ref. 6) are shown for comparison. The dotted line is a guide to the eye.

results indicate that the short- and intermediate-range structures are very similar between bulk silica and silica nanoparticles at least in terms of $S(Q)$. With increasing pressure of up to 7.4 GPa, we see substantial changes in $S(Q)$, especially at $Q < 5 \text{ \AA}^{-1}$. For example, the intensity of the first sharp diffraction peak (FSDP) decreases by $\sim 20\%$ while its position shifts from 1.52 to 1.90 \AA^{-1} ; a new peak appears at $\sim 3.0 \text{ \AA}^{-1}$. These pressure-induced changes in $S(Q)$ are basically similar to those previously reported for bulk silica glass.^{6,18} As shown in Fig. 2, however, the pressure-induced shifts in the position of the FSDP at room temperature are more significant in the present $\alpha\text{-SiO}_2$ nanoparticles than those in bulk silica glass.⁶ Furthermore, the observed shifts are almost comparable to those observed for bulk silica glass under high temperature and pressure,⁶ indicating that a decrease in particle size and an increase in temperature have a

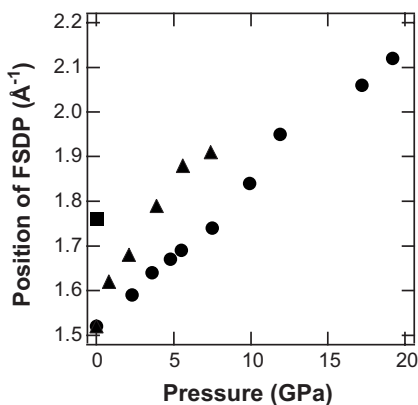


FIG. 2. The position of the FSDP measured for amorphous silica nanoparticles between 0.1 MPa and 7.4 GPa (filled triangles) and that of the pressure retrieved sample from 7.4 GPa (filled square). The data for bulk silica glass between 0.1 MPa and 19.2 GPa (filled circles) (Ref. 6) are shown for comparison.

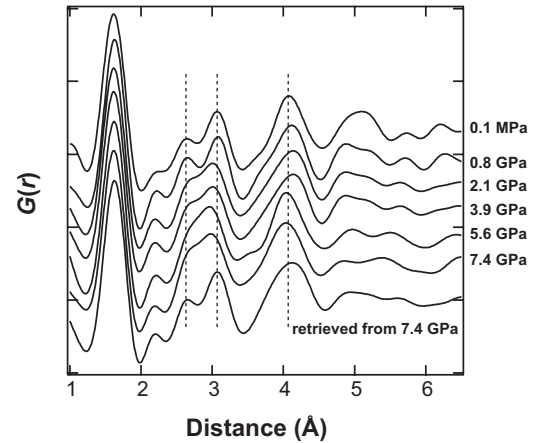


FIG. 3. The average pair correlation function $G(r)$ for amorphous silica nanoparticles at pressures of up to 7.4 GPa and that of the pressure retrieved sample from 7.4 GPa. The dotted lines are a guide to the eye.

comparable effect in reducing transformation pressure. It should also be noted that the position of the FSDP of the silica nanoparticles compressed at 7.4 GPa does not return to the original value (1.52 \AA^{-1}) after releasing the pressure. The FSDP of the sample retrieved from 7.4 GPa is located at 1.76 \AA^{-1} , which almost corresponds to the highest achievable Q value that is observed in the permanently densified bulk silica glass ($\sim 20\%$ densified) that is formed by compression at 16–18 GPa at room temperature^{24,25} or by compression at 7.4 GPa at a temperature of $700 \text{ }^\circ\text{C}$.⁶ These results demonstrate that silica nanoparticles exhibit pressure-induced structural changes that lead to a permanent densification at much lower pressures and temperatures, which occurs in bulk silica glass.

We next estimate the real-space structural changes in silica nanoparticles under high pressures from the Fourier sine transform of the structure factor (see Fig. 3),

$$G(r) = \frac{2}{\pi} \int Q[S(Q) - 1] \sin(Qr) M(Q) dQ, \quad (1)$$

where $M(Q)$ is a modification function to reduce termination effects resulting from the finite upper limit of Q .²⁶ At ambient pressure, we see five discernible peaks at 1.61 , 2.64 , 3.07 , 4.09 , and 5.10 \AA , which are attributed to the Si-O (first shell), O-O (first shell), Si-Si (first shell), Si-O (second shell), and O-O and Si-Si (second shell) pairs, respectively, which are similar to the case of $G(r)$ in bulk silica glass.²⁷ Between 0.1 MPa and 7.4 GPa, the first neighbor Si-O and O-O separations are hardly changed within the resolution of our analysis. However, a substantial shortening in the first neighbor Si-Si distance can be seen in $G(r)$ under the applied pressure. In addition, the peak that is located at $\sim 5 \text{ \AA}$ is significantly reduced in intensity during compression. These observed changes in $G(r)$ of silica nanoparticles suggest that volume compression below 7.4 GPa will not alter the coordination environment of the SiO_4 units but will only induce a decrease in Si-O-Si intertetrahedral angles, as manifested by a decrease in the first neighbor Si-Si distance.

We next turn to $G(r)$ of the pressure quenched sample. We see from Fig. 3 that as far as the distance region below ~ 3.5 Å is concerned, $G(r)$ of the pressure quenched sample is nearly comparable to that of the uncompressed sample, indicating that the pressure-induced changes in the Si-O-Si intertetrahedral angles are almost restored to the original values after releasing the applied pressure. However, the peak at ~ 4 Å, which is ascribed to the Si-O second shell, of the pressure quenched sample becomes rather broad as compared to that of the uncompressed sample, and the peak at ~ 5 Å, which results from the O-O and Si-Si second shells, of the former sample was significantly reduced in intensity. These results elucidate that for silica nanoparticles, the pressure-induced deformation of the network connectivity in length scale from ~ 4 to ~ 6 Å is not completely restored after releasing the pressure from 7.4 GPa to atmospheric pressure. This modification of the real-space correlations in the intermediate-range length scale most likely explains the corresponding change in the position of the FSDP of the pressure quenched sample since it has been recognized that the FSDP in a -SiO₂ mainly results from the spatial correlations in length scales typical of intermediate-range order (IRO).²⁸ In particular, an appreciable decrease in the real-space correlations at a distance $> \sim 5$ Å in the pressure quenched sample will be mainly responsible for the observed shift to a higher Q (1.76 Å⁻¹) in the FSDP.²⁹ A similar shift to higher Q values in the FSDP with increasing applied pressure can also be interpreted in terms of the substantial decrease in the real-space correlations longer than ~ 5 Å.

As mentioned earlier, some crystalline materials, e.g., CeO₂,¹¹ γ -Fe₂O₃,¹² and rutile (TiO₂),¹³ display a lower phase transition pressure with a decrease in particle size, which is similar to the case of the present a -SiO₂ system. The reduction in transition pressure in the pressure-induced solid-solid phase transformation in these crystals has been explained in terms of homogeneous nucleation and growth of a high-pressure phase in a low-pressure-phase matrix, which was accompanied by a large collapse in volume upon phase transformation.¹¹⁻¹³ Assuming that the interfacial free energy σ between two phases is isotropic, one can obtain the nucleation barrier ΔG^* for a spherically grown nucleus as follows:^{11,30}

$$\Delta G^* = \frac{16\pi\sigma^3}{3(\Delta G_m - \Delta G_s)^2 \rho_l^2}, \quad (2)$$

where ΔG_m and ΔG_s are a free-energy reduction and a misfit strain energy per unit mass of the newly created high-pressure phase, respectively, and ρ_l is the density of the low-pressure phase. Since the nucleation rate is proportional to $\exp[-\Delta G^*/kT]$, one sees from Eq. (2) that the driving force of the phase transition is ΔG_m , which is given by³⁰

$$\Delta G_m = U^l - U^h - T(S^l - S^h) + P(V^l - V^h). \quad (3)$$

Here, U^i , S^i , and V^i ($i=l, h$) are the internal energies, entropies, and volumes per unit mass of the low (l) or the high (h)

pressure phase, respectively. It is quite likely that $U^l - U^h$ and $S^l - S^h$ are similar between nanoparticles and the corresponding bulk material.¹¹ Thus, the large volume change, $\Delta V = V^l - V^h$, in Eq. (3) is considered to be responsible for the reduced transformation pressure in the nanophase crystalline materials.¹¹⁻¹³

We propose that the above scenario of phase transformation can be applied to the pressure-induced structural transformation of a -SiO₂ since the polymorphic transition in amorphous solids can be regarded as a transformation between two structural states in the IRO.⁴ As shown in Fig. 2, the pressure-induced shift in the position of FSDP is more significant in the silica nanoparticles than in the bulk silica, suggesting a larger pressure-induced change in the IRO in the former material than that in the latter. This structural modification is most likely accompanied by a large volume collapse as well. As for the bulk silica glass, a discontinuous volume change of about 20% upon transformation was indeed observed.⁷ We therefore suggest that the expected volume collapse resulting from the transformation between different IRO structural states accounts for the reduction in the transition pressure of silica nanoparticles. If the strain energy term ΔG_s in Eq. (2) is dominant, an elevation of phase transformation pressure in nanocrystals, such as CdSe (Ref. 8) and PbS,⁹ will occur. In amorphous materials, however, the contribution from the surface strain energy term ΔG_s will not be significantly low because the boundary between two IRO structural states may not be well defined. Thus, we consider that the size dependence of the pressure-induced structural transformations in a -SiO₂ is mainly governed by the pressure-volume part of a free-energy reduction.

In conclusion, we have demonstrated that in silica nanoparticles, the permanent transformation between different IRO structural states takes place at lower pressures than what occurs in the corresponding bulk at room temperature. Similar to the case of the phase transition that occurs in some crystalline materials, a larger volume change upon transformation accounts for the reduced transformation pressure in silica nanoparticles. In a -SiO₂, the first-order amorphous-amorphous transition is believed to be kinetically hindered at least at room temperature.³ However, the present results suggest that the transformation pressure of silica nanoparticles are thermodynamically rather than kinetically controlled, which is similar to the case of LDA-HDA transitions observed in amorphous ice systems.⁵ Thus, the present observations not only provide a window to create high-pressure forms of amorphous solids but also may imply the appearance of a first-order-like, or thermodynamically controlled, transition pathway just by reducing the size, even at room temperature.

The synchrotron radiation experiments were performed at the SPring-8 with the approval of the Japan Synchrotron Radiation Research Institute (Proposal No. 2003B0457-ND2a-np-Na).

- ¹M. Guthrie, C. A. Tulk, C. J. Benmore, J. Xu, J. L. Yarger, D. D. Klug, J. S. Tse, H.-K. Mao, and R. J. Hemley, *Phys. Rev. Lett.* **93**, 115502 (2004).
- ²Y. Katayama, T. Mizutani, W. Utsumi, O. Shinomura, M. Yamakata, and K. Funakoshi, *Nature (London)* **403**, 170 (2000).
- ³D. J. Lacks, *Phys. Rev. Lett.* **84**, 4629 (2000).
- ⁴M. C. Wilding, M. Wilson, and P. F. McMillan, *Chem. Soc. Rev.* **35**, 964 (2006), and references therein.
- ⁵O. Mishima, L. D. Calvert, and E. Whalley, *Nature (London)* **314**, 76 (1985); O. Mishima, *J. Chem. Phys.* **100**, 5910 (1994).
- ⁶Y. Inamura, Y. Katayama, W. Utsumi, and K. I. Funakoshi, *Phys. Rev. Lett.* **93**, 015501 (2004).
- ⁷G. D. Mukherjee, S. N. Vaidya, and V. Sugandhi, *Phys. Rev. Lett.* **87**, 195501 (2001).
- ⁸S. H. Tolbert and A. P. Alivisatos, *Science* **265**, 373 (1994).
- ⁹S. B. Qadri, J. Yang, B. R. Ranta, E. F. Skelton, and J. Z. Hu, *Appl. Phys. Lett.* **69**, 2205 (1996).
- ¹⁰S. B. Qadri, E. F. Skelton, A. D. Dinsmore, J. Z. Hu, W. J. Kim, C. Nelson, and B. R. Ranta, *J. Appl. Phys.* **89**, 115 (2001).
- ¹¹J. Z. Jiang, J. S. Olsen, L. Gerward, and S. Mørup, *Europhys. Lett.* **44**, 620 (1998).
- ¹²Z. Wang, S. K. Saxena, V. Pischedda, H. P. Liermann, and C. S. Zha, *J. Phys.: Condens. Matter* **13**, 8317 (2001).
- ¹³Z. Wang, S. K. Saxena, V. Pischedda, H. P. Liermann, and C. S. Zha, *Phys. Rev. B* **64**, 012102 (2001).
- ¹⁴L. Stixrude, in *Structure and Imperfections in Amorphous and Crystalline Silicon Dioxide*, edited by R. A. B. Devine, J.-P. Duraud, and E. Dooryhée (Wiley, Chichester, 2000), pp. 69–103.
- ¹⁵P. W. Bridgman and I. Simon, *J. Appl. Phys.* **24**, 405 (1953).
- ¹⁶M. Grimsditch, *Phys. Rev. Lett.* **52**, 2379 (1984).
- ¹⁷R. J. Hemley, H. K. Mao, P. M. Bell, and B. O. Mysen, *Phys. Rev. Lett.* **57**, 747 (1986).
- ¹⁸C. Meade, R. J. Hemley, and H. K. Mao, *Phys. Rev. Lett.* **69**, 1387 (1992).
- ¹⁹J. Arndt and D. Stöffler, *Phys. Chem. Glasses* **10**, 117 (1969).
- ²⁰P. McMillan, B. Piriou, and R. Couty, *J. Chem. Phys.* **81**, 4234 (1984).
- ²¹T. Uchino, A. Sakoh, M. Azuma, S. Kohara, M. Takahashi, M. Takano, and T. Yoko, *Phys. Rev. B* **67**, 092202 (2003).
- ²²C. C. Liu and G. E. Maciel, *J. Am. Chem. Soc.* **118**, 5103 (1996).
- ²³T. Uchino, A. Aboshi, S. Kohara, Y. Ohishi, M. Sakashita, and K. Aoki, *Phys. Rev. B* **69**, 155409 (2004).
- ²⁴S. Susman, K. J. Volin, R. C. Liebermann, G. D. Gwanmesia, and Y. Wang, *Phys. Chem. Glasses* **31**, 144 (1990).
- ²⁵S. Sugai and A. Onodera, *Phys. Rev. Lett.* **77**, 4210 (1996).
- ²⁶E. A. Lorch, *J. Phys. C* **2**, 229 (1969).
- ²⁷H. F. Poulsen, J. Neufelnd, H.-B. Neumann, J. R. Schneider, and M. D. Zeidler, *J. Non-Cryst. Solids* **188**, 63 (1995).
- ²⁸S. R. Elliott, *Nature (London)* **354**, 445 (1991); *Phys. Rev. Lett.* **67**, 711 (1991).
- ²⁹T. Uchino, J. D. Harrop, S. N. Taraskin, and S. R. Elliott, *Phys. Rev. B* **71**, 014202 (2005).
- ³⁰D. A. Porter and K. E. Easterling, *Phase Transformation in Metals and Alloys*, 2nd ed. (Chapman and Hall, London, 1992).